

Predicting Severity of *C. difficile* Infections from the Taxonomic Composition of the Gut Microbiome

Kelly L. Sovacool¹, Sarah E. Tomkovich², Megan L. Coden³, Jenna Wiens⁵, Vincent B. Young^{2,4}, Krishna Rao⁴, and Patrick D. Schloss^{2,6,†}

¹Department of Computational Medicine & Bioinformatics, University of Michigan

²Department of Microbiology & Immunology, University of Michigan

³Department of Molecular, Cellular, and Developmental Biology, University of Michigan

⁴Division of Infectious Diseases, Department of Internal Medicine, University of Michigan

⁵Department of Electrical Engineering & Computer Science, University of Michigan

⁶Center for Computational Medicine and Bioinformatics, University of Michigan

Compiled June 7, 2023

†Correspondence: pschloss@umich.edu.

ABSTRACT *Clostridioides difficile* infection (CDI) can lead to adverse outcomes including ICU admission, colectomy, and death. The composition of the gut microbiome plays an important role in determining colonization resistance and clearance upon exposure to *C. difficile*. We investigated whether machine learning (ML) models trained on 16S rRNA gene amplicon sequences from gut microbiota extracted from 1,277 patient stool samples on the day of CDI diagnosis could predict which CDI cases led to severe outcomes. We then trained ML models to predict CDI severity on OTU relative abundances according to four different severity definitions: the IDSA severity score on the day of diagnosis, all-cause adverse outcomes within 30 days, adverse outcomes confirmed as attributable to CDI via chart review, and a pragmatic definition that uses the attributable definition when available and otherwise uses the all-cause definition. The models predicting pragmatic severity performed best, suggesting that while chart review is valuable to verify the cause of complications, including as many samples as possible is indispensable for training performant models on imbalanced datasets. Permutation importance identified *Enterococcus* as the most important OTU for model performance, and increased relative abundance of *Enterococcus* was associated with severe outcomes. Finally, we evaluated the potential clinical value of the OTU-based models and found similar performance compared to prior models based on Electronic Health Records. The modest performance of the OTU-based models represents a step toward the goal of deploying models to inform clinical decisions and ultimately improve CDI outcomes.

KEYWORDS: *C. difficile* infection, supervised machine learning, gut microbiome, amplicon sequencing

INTRODUCTION

Clostridoides difficile infection (CDI) is the most common nosocomial infection in the United States, and community-acquired cases are on the rise (1, 2). The classic CDI case typically occurs soon after antibiotic use, which perturbs the protective gut microbiota and allows *C. difficile* to proliferate (3). Non-antibiotic medications including proton-pump inhibitors and osmotic laxatives have also been associated with increased CDI susceptibility and inhibited clearance (4, 5). Diarrhea is the primary symptom, with some patients developing colitis, toxic megacolon, or requiring intensive care with an in-hospital mortality rate of approximately 8-9% (6, 7). Furthermore, 5-20% of initial cases reoccur within 2-8 weeks, and recurrent cases are associated with increased morbidity and mortality risk (8, 3). Patient risk factors for CDI-related morbidity and mortality include age greater than 65 years, history of recurrent CDI, and co-morbid chronic illnesses (9). CDI remains a significant burden on the US health care system with approximately 500,000 cases annually (10, 11).

There is a need for robust, accurate methods to identify patients at risk of severe CDI outcomes. When paired with treatment options that may reduce risk of severity, prediction models can guide clinician decision-making to improve patient outcomes while minimizing harms from unnecessary treatment. Numerous scoring systems for predicting severe CDI outcomes based on patient clinical factors have been developed, but none have validated well to external datasets nor are any in use in routine clinical practice (12, 13). Rather than relying on limited sets of human-curated variables, machine learning (ML) is a promising approach that allows for use of thousands of features to classify samples and predict outcomes. Indeed, ML models trained on entire Electronic Health Record (EHR) data have demonstrated improved performance over curated models (14, 15).

Aside from patient factors encoded in EHRs, the state of the patient gut microbiome is a promising factor to predict severity, as the host microbiota can play either a protective or harmful role in *C. difficile* colonization, infection, and clearance. Mouse studies have found that the initial taxonomic composition of the gut microbiome predicts differences in clearance, moribundity, and cecal tissue damage in mice infected with CDI (16, 17). Identifying features of the human gut microbiota that promote or prevent severe infections can guide further experiments to elucidate microbial mechanisms of CDI severity, and incorporating these features into CDI severity models may improve model performance to help guide clinical treatment decisions.

We set out to investigate whether ML models trained on the taxonomic composition of the gut microbiome can predict CDI severity in a human cohort, whether the severity definition employed affects model performance, and whether there is potential clinical value in deploying OTU-based models. Stool samples from 1,277 CDI patients were collected on the day

of diagnosis and 16S rRNA gene amplicon sequencing was performed, followed by clustering sequences into Operational Taxonomic Units (OTUs). We then trained ML models to classify or predict each of four severity definitions from OTU relative abundances, identified which microbial features contributed most to model performance, and conducted a proof-of-concept analysis of the potential clinical value of these OTU-based models and compared these to prior EHR-based models.

RESULTS

CDI severity. There is not currently a consensus definition of CDI severity. Some scoring systems leverage clinical data available during the course of CDI, while others focus on adverse outcomes of CDI at 30 days after diagnosis (9, 18). We explored four different ways to define CDI cases as severe or not (Figure 1). The Infectious Diseases Society of America (IDSA) definition of severe CDI is based on laboratory values collected on the day of diagnosis, with a case being severe if serum creatinine level is greater than or equal to 1.5mg/dL and the white blood cell count is greater than or equal to $15\text{k}/\mu\text{L}$ (19). Although data for the IDSA score is straightforward to collect, it is known to be a poor predictor of adverse outcomes (20). The remaining definitions we employed focus on the occurrence of adverse outcomes, which may be more clinically relevant. The “attributable” severity definition is based on disease-related complications defined by the Centers for Disease Control and Prevention, where an adverse event of ICU admission, colectomy, or death occurs within 30 days of CDI diagnosis, and the adverse event is determined to be attributable to the CDI by physician chart review (21). However, physician chart review is time-consuming and has not been completed for all cases ($n=46$ out of 86 cases with an adverse outcome), so we defined “all-cause” severity where a case is severe if an adverse event occurs within 30 days of the diagnosis regardless of the cause of the adverse event. Finally, we defined a “pragmatic” severity definition that makes use of the attributable definition when available and uses the all-cause definition when chart review has not been completed, allowing us to use as many samples as we have available while taking physicians’ expert opinions into account where possible (Figure 1 B). We trained ML models to classify (in the case of the IDSA definition) or predict (in the case of the three other definitions) severity and determined how well OTU-based models perform for each definition.

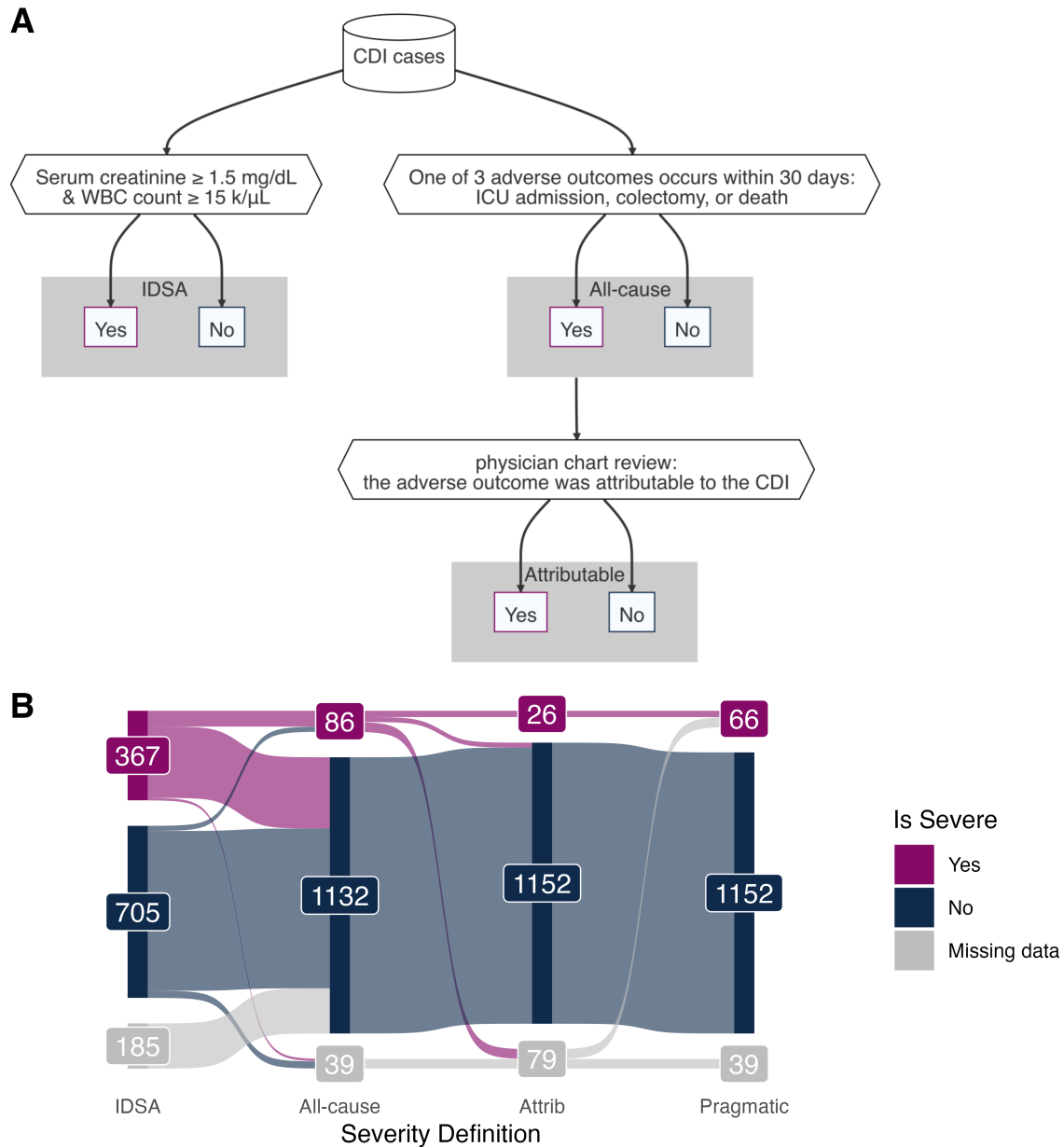


FIG 1 CDI severity definitions. A) Decision flow chart to define CDI cases as severe according to the Infectious Diseases Society of America (IDSA) based on lab values, the occurrence of an adverse outcome due to any cause (All-cause), and the occurrence of disease-related complications confirmed as attributable to CDI with chart review (Attributable). **B)** The proportion of severe CDI cases labelled according to each definition. An additional 'Pragmatic' severity definition uses the Attributable definition when possible, and falls back to the All-cause definition when chart review is not available. See Table 1 for sample counts and proportions of severe cases across severity definitions.

TABLE 1 Sample counts and proportion of severe cases. Each severity definition has a different number of patient samples available, as well as a different proportion of cases labelled as severe.

(a) Full datasets

Severity	n	% severe
All-cause	1,218	7.1
Attributable	1,178	2.2
IDSA	1,072	34.2
Pragmatic	1,218	5.4

(b) Intersection of samples with all labels available

Severity	n	% severe
All-cause	993	4.6
Attributable	993	2.6
IDSA	993	32.7
Pragmatic	993	2.6

Model performance. We first set out to train the best models possible for each severity definition. Not all samples have outcomes available for all four severity definitions due to missing data for some patient lab values and incomplete chart review (Figure 1 B), thus each severity definition had a different number of samples when using as many samples as possible (Table 1 A). We referred to these as the full datasets. Random forest models were trained on 100 splits of the datasets into training and test sets, and performance was evaluated on the held-out test set using the area under the receiver-operator characteristic curve (AUROC). Since the severity outcomes were highly imbalanced with different proportions of severe samples between definitions, we also calculated the balanced precision and the area under the balanced precision-recall curve (AUBPRC) as first proposed by Wu et al. (22) to describe the precision that would be expected if the outcomes were balanced.

After training on the full datasets, the performance as measured by the AUROCs of the training set cross-validation folds were similar to those of the held-out test sets, indicating that the models are neither overfit nor underfit (Figure 2 A). As measured by AUROC on the held-out test sets, models predicting pragmatic severity performed best with a median AUROC of 0.69, and this was significantly different from that of the other definitions on the full datasets ($P < 0.05$). Models predicting IDSA, all-cause, and attributable severity performed similarly with median test set AUROCs of 0.61, 0.63, and 0.61 respectively. The test set AUROCs were not significantly different ($P > 0.05$) for attributable and IDSA nor for attributable and all-cause, but the IDSA and all-cause AUROCs were significantly different from each other ($P < 0.05$). We plotted the receiver-operator characteristic curve and found that the pragmatic severity models outperformed the others at all specificity values (Figure 2 B). For comparison, a prior study with a different dataset trained a logistic regression model on whole Electronic Health Record data extracted on the day of CDI diagnosis to predict attributable severity, yielding an AUROC of 0.69 (15). While our attributable severity model did not meet this performance, the pragmatic severity model performed just as well as the EHR-based model in terms of AUROC.

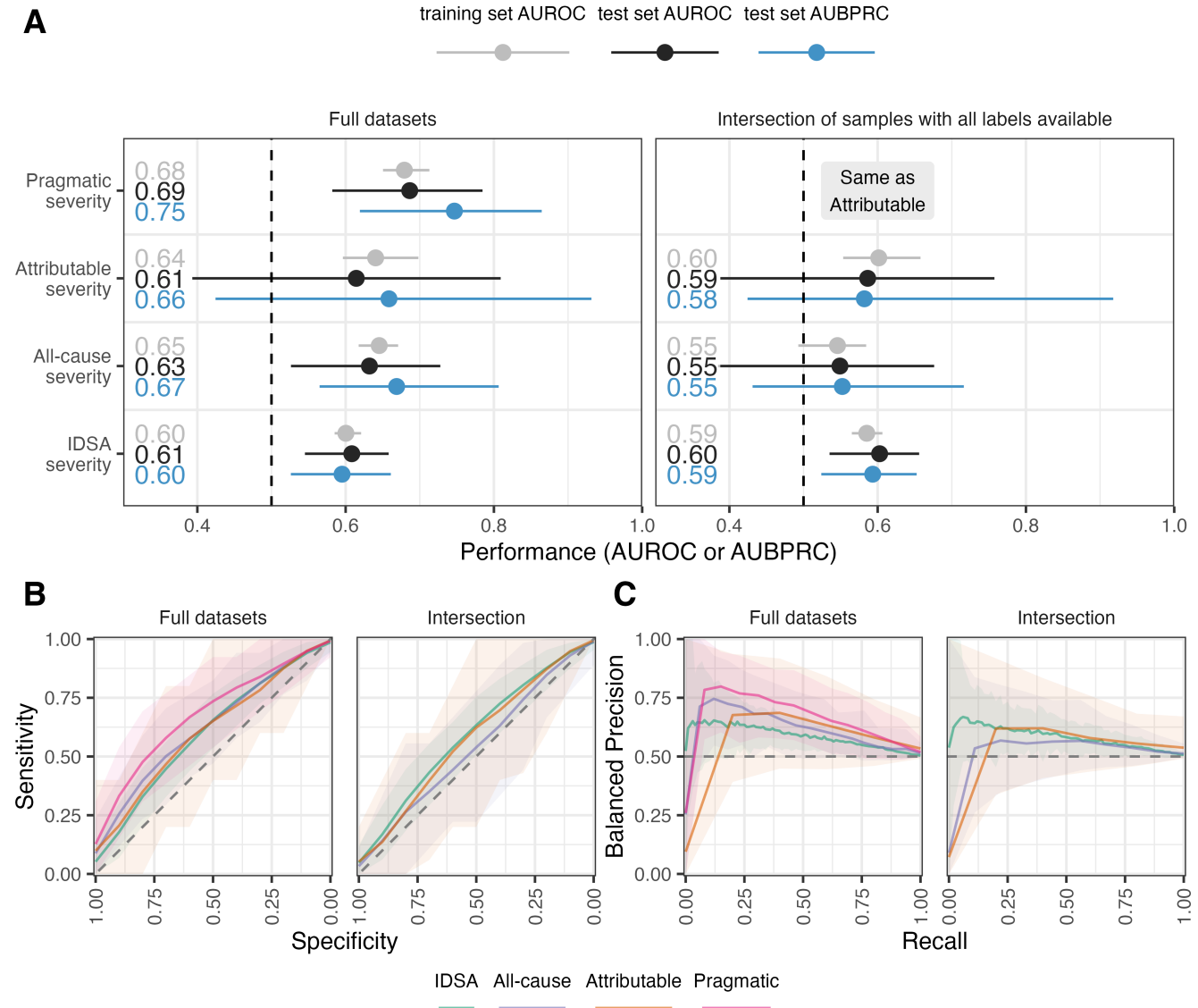


FIG 2 Performance of ML models. In the left facets, models were trained on the full datasets, with different numbers of samples available for each severity definition. In the right facets, models were trained on the same dataset consisting of the intersection of samples with labels available for all definitions. Note that the intersection dataset has exactly the same labels for attributable and pragmatic severity, thus these have identical performance. **A)** Area under the receiver-operator characteristic curve (AUROC) for the test sets and cross-validation folds of the training sets, and the area under the balanced precision-recall curve (AUBPRC) for the test sets. Each point is annotated with the median performance across 100 train/test splits with tails as the 95% CI. **B)** Receiver-operator characteristic curves for the test sets. Mean specificity is reported at each sensitivity value, with ribbons as the 95% CI. **C)** Balanced precision-recall curves for the test sets. Mean balanced precision is reported at each recall (sensitivity) value, with ribbons as the 95% CI. Original unbalanced precision-recall curves are shown in Supplementary Figure 4.

Since the data are highly imbalanced with only a small proportion of CDI cases having a severe outcome, evaluating the trade-off between precision and recall is more informative than the receiver-operator characteristic because precision and recall do not consider true negatives, which may overinflate the AUROC. However, unlike for AUROC, the baseline for the area under the precision-recall curve depends on the proportion of positive outcomes (i.e. severe cases) in the data, which vary across these severity definitions. To allow comparison of precision across datasets with different proportions of positives, Wu et al. (22) introduced the concept of balanced precision, a transformation of precision based on Bayes' theorem that represents the precision that would have been expected if the proportion of positives were balanced at 0.5. Reporting the area under the balanced precision-recall curve (AUBPRC) allows us to compare the trade-off between precision and recall for our different severity definitions. The test set median AUBPRCs from the full datasets followed a similar pattern as the test set AUROCs with 0.60 for IDSA severity, 0.67 for all-cause severity, 0.66 for attributable severity, and 0.75 for pragmatic severity. The AUBPRCs were significantly different from each other ($P < 0.05$) for each pair of severity definitions except for attributable versus all-cause. We plotted the balanced precision-recall curve and found that the IDSA definition outperformed all other models at very low recall values, but the others outperform IDSA at all other points of the curve (Figure 2 C). The 95% confidence intervals overlapped the baseline AUROC and AUBPRC for the attributable severity models, while all others did not overlap the baseline.

While it is advantageous to use as much data as available to train the best models possible, comparing performances of models trained on different subsets of the data is not entirely fair. To enable fair comparisons of the model performances across different severity definitions, we also selected the intersection of samples ($n=993$) that had labels for all four severity definitions and repeated the model training and evaluation process on this intersection dataset. The attributable definition is exactly the same as the pragmatic definition for the intersection dataset, as we defined pragmatic severity to use the attributable definition when available. The performance results on the intersection dataset are shown in the right facets of each panel of Figure 2.

As with the full datasets, the AUROCs of the training sets and test sets were similar within each severity definition. The median test set AUROCs were 0.60 for IDSA severity, 0.55 for all-cause severity, 0.59 and for attributable severity. The AUROCs on the intersection dataset were significantly different for all-cause versus attributable and all-cause versus IDSA severity ($P < 0.05$), but not for IDSA versus attributable severity ($P > 0.05$). The median test set AUBPRCs were 0.59 for IDSA severity, 0.55 for all-cause severity, 0.58 and for attributable severity. Just as with the AUROCs, the AUBPRCs were significantly different for all-cause versus attributable and all-cause versus IDSA severity ($P < 0.05$), but not for IDSA

versus attributable severity ($P > 0.05$). For all severity definitions, performance dropped between the full dataset and the intersection dataset since fewer samples are available, but this effect is least dramatic for IDSA severity as the full and intersection datasets are more similar for this definition (Table 1 B). The 95% confidence interval overlaps with the baseline for both AUROC and AUPRC for all definitions on the intersection dataset except for IDSA severity.

Feature importance. We performed permutation feature importance to determine which OTUs contributed the most to model performance. An OTU was considered important if performance decreased when it was permuted in at least 75% of the train/test splits, with greater differences in AUROC meaning greater importance. We plotted mean decrease in AUROC alongside \log_{10} -transformed mean relative abundances for the top OTUs (Figure 3). *Enterococcus* was the most important OTU, being significantly important for all models except for attributable severity on the full dataset. *Staphylococcus* was important for the pragmatic and all-cause definitions on the full datasets, but not for models trained on the intersection dataset. *Lactobacillus* was important only for the all-cause definition on the intersection dataset. All remaining OTUs had differences in AUROC < 0.02 and were only significantly important in one or two of the models at most. There is not always a clear pattern of increased or decreased relative abundance for important OTUs in severe CDI cases, but all of the top 5 OTUs had an increased mean relative abundance in severe cases relative to not severe cases.

Estimating clinical value. Even if a model performs well, it may not be useful in a clinical setting unless it can guide clinicians to choose between treatment options. At this time, we are not aware of any direct evidence that a particular treatment reduces the risk of severe CDI outcomes. However, with some assumptions we offer a proof-of-concept analysis of the potential clinical value of OTU-based severity prediction models when paired with treatments that may reduce severity. When considering the suitability of a model for deployment in clinical settings, the number needed to screen (NNS) is a highly relevant metric representing how many patients must be predicted as severe by the model to identify one true positive. Similarly, the number needed to treat (NNT) is the number of true positive patients that must be treated by an intervention in order for one patient to benefit from the treatment. Multiplying NNS by NNT yields the number needed to benefit (NNB): the number of patients predicted to have a severe outcome who then benefit from the treatment (23). Thus the NNB pairs model performance with treatment effectiveness to estimate the benefit of using predictive models in clinical practice, and are useful for comparing models and performing cost-benefit analyses. Lower values of NNS, NNT, and NNB are better, with the minimum value being 1, as fewer patients must be screened and treated in order to benefit a single patient.

Current clinical guidelines specify vancomycin and fidaxomicin as the standard antibiotics to treat CDI, with a pref-

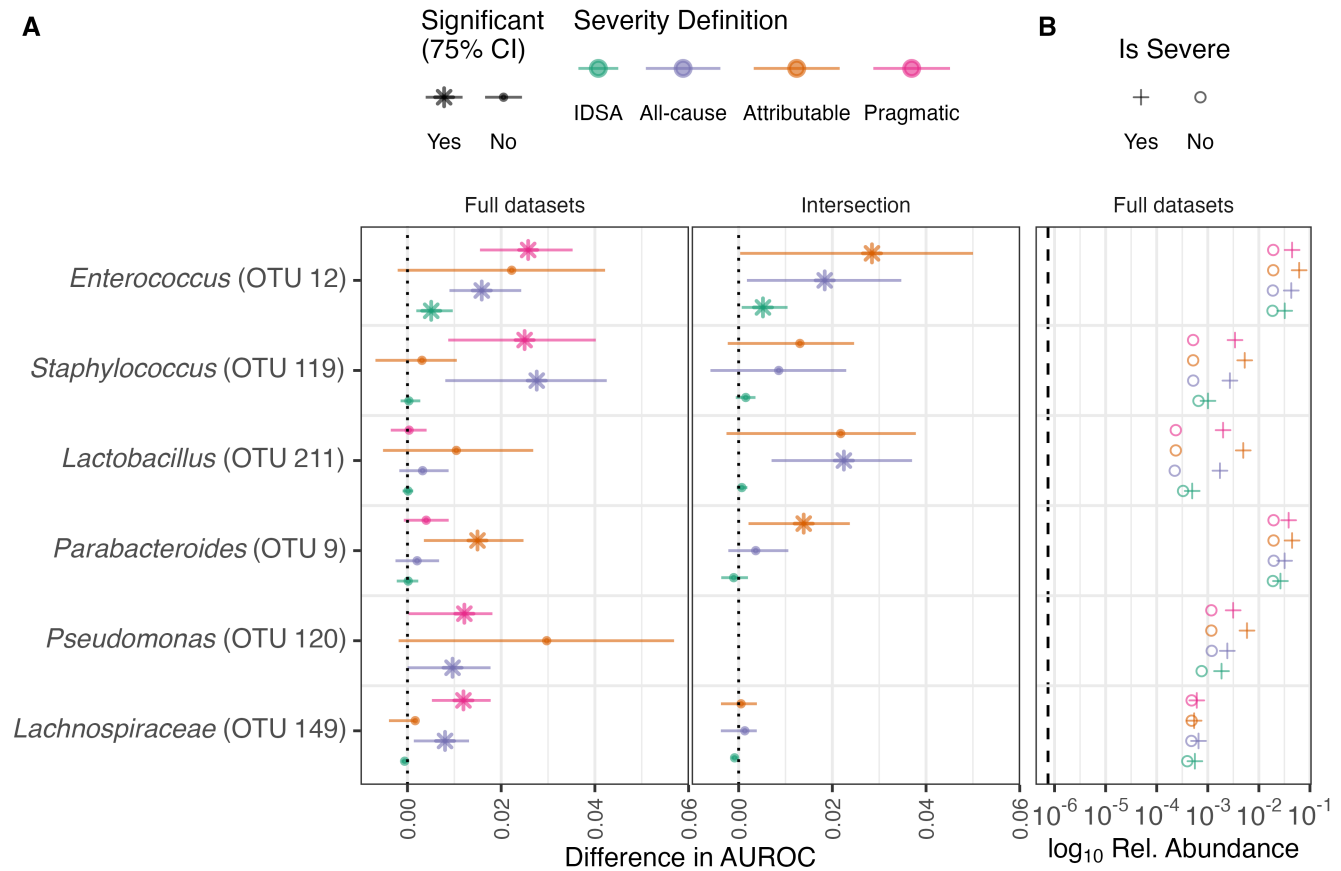


FIG 3 Most important OTUs for model performance. A) Feature importance via permutation test. For each OTU, the order of samples was randomized in the test set 100 times and the AUROC was re-calculated to estimate the permutation performance. OTUs with a greater difference in AUROC (actual performance minus permutation performance) are more important. Mean difference in AUROC and the 75% confidence interval (CI) is reported for each OTU that had a mean difference ≥ 0.01 for at least one severity definition, with starred OTUs being significant for the 75% CI. Notably, the OTU most likely corresponding to *C. difficile* was not important (see Supplementary Figure 5). Left: models were trained on the full datasets, with different numbers of samples available for each severity definition. Right: models were trained on the intersection of samples with all labels available for each definition. Note that Attributable and Pragmatic severity are exactly the same for the intersection dataset. *Pseudomonas* (OTU 120) is not shown for IDSA severity in the full datasets nor in the intersection dataset because it was removed during pre-processing due to having near-zero variance. **B)** Log₁₀-transformed mean relative abundances of the most important OTUs on the full datasets, grouped by severity (shape). The vertical dashed line is the limit of detection.

erence for fidaxomicin due to its higher rate of sustained resolution of CDI and lower rate of recurrence (24). The NNTs of fidaxomicin for sustained resolution and prevention of recurrence are each estimated to be 10 (25, 26). However, fidaxomicin is considerably more expensive than vancomycin. If fidaxomicin were shown to reduce the risk of severe CDI outcomes, it could be preferentially prescribed to patients predicted to be at risk, while prescribing vancomycin to low-risk patients. If we assume that the superior efficacy of fidaxomicin for sustained resolution and reduced recurrence also translates to reducing the risk of severe outcomes, we can pair the NNT of fidaxomicin with the NNS of OTU-based prediction models to estimate the NNB.

To calculate a clinically-relevant NNS for these models, we computed the confusion matrix at the 95th percentile of risk for each prediction model. We excluded the IDSA severity models as the IDSA severity scores were calculated on the day of diagnosis, thus they are classification rather than prediction problems. Furthermore, IDSA severity scores do not correlate well with disease-related adverse events which are a more salient outcome to prevent. Among the models predicting severe outcomes, those trained on the full datasets performed best with an NNS of 4 for the all-cause definition, 6 for the attributable definition, and 3 for the pragmatic definition (Table 2). Multiplying the NNS of the OTU-based models by the estimated NNT of 10 for fidaxomicin yields NNB values of 40 for all-cause severity, 60 for attributable severity, and 30 for pragmatic severity. Thus, in a hypothetical scenario where these assumptions about fidaxomicin hold true, between 30 and 60 patients would need to be predicted to experience a severe outcome and be treated with fidaxomicin in order for one patient to benefit, with the pragmatic severity models having the best NNB when paired with fidaxomicin. As the NNS values were computed at the 95th percentile of risk (where 5% of patients screened are predicted to experience severity), these NNB values mean that 600 to 1,200 total CDI patients would need to be screened by an OTU-based prediction model and treated with fidaxomicin in order for one patient to benefit. For comparison, prior studies predicted CDI-attributable severity using whole Electronic Health Record data extracted two days after diagnosis and from a smaller set of manually curated variables, achieving precision values of 0.417 (NNS = 2.4) for the EHR model and 0.167 (NNS = 6.0) for the curated model at the 95th percentile of risk (15, 14). Pairing the prior EHR-based model with fidaxomicin would yield an NNB of 24 with 480 total CDI patients screened and treated for one patient to benefit. Thus the pragmatic severity model did not outperform the EHR-based model, although the EHR data were extracted two days after diagnosis while OTUs in this study are from stool samples collected on the day of diagnosis. These estimates represent a proof-of-concept demonstration of the potential value and trade-offs of deploying severity prediction models trained on microbial factors versus EHRs to guide clinicians' treatment decisions.

TABLE 2 Predictive model performance at 95th percentile of risk. The confusion matrix was computed for the decision threshold at the 95th percentile of risk for each severity prediction model, which corresponds to 5% of cases predicted to have a severe outcome. The number needed to screen (NNS) to identify one true positive is the reciprocal of precision.

(a) Full datasets

Outcome	Risk threshold	TP	FP	TN	FN	Precision	NNS	Recall	Specificity
All-cause	0.20	3	9	217	14	0.25	4	0.18	0.96
Attributable	0.10	2	10	220	3	0.17	6	0.40	0.96
Pragmatic	0.25	4	8	222	9	0.33	3	0.31	0.97

(b) Intersection of samples with all labels available

Outcome	Risk threshold	TP	FP	TN	FN	Precision	NNS	Recall	Specificity
All-cause	0.2	2	8	181	7	0.2	5	0.22	0.96
Attributable	0.1	1	9	184	4	0.1	10	0.20	0.95

DISCUSSION

We trained ML models based on gut microbial communities on the day of CDI diagnosis to predict CDI severity according to four different severity definitions. The purpose of the full datasets was to train the best models possible given the constraints, while using the intersection dataset allows for comparing severity definitions. We found that models predicting pragmatic severity with as much data as available performed best, while models classifying IDSA severity outperformed the all-cause and attributable definitions only with the intersection. Performance dropped substantially when reducing to the intersection dataset for all definitions, likely due to the particularly imbalanced nature of the all-cause and attributable definitions. These results demonstrate the importance of using as many samples as possible when data are sparse and the outcome is low prevalence, as well as the need to incorporate physician's expertise when possible.

Permutation feature importance revealed patterns of important bacteria that concord with the literature. Enrichment of *Enterococcus* and *Lactobacillus* in *C. difficile* infection and severity have been well-documented in prior studies, thus their importance and increase in abundance for severe cases is not surprising (27, 28, 29, 17). For many of the top OTUs, there is a wide range in importance. Notably, the OTU represented by *Pseudomonas* had wide variance in importance for the full dataset in models predicting attributable severity, with the maximum point more important than any other OTU yet a minimum below zero. However, for the intersection dataset, this OTU was removed due to having near-zero variance. The presence of *Pseudomonas* was thus informative in a small number of patient samples, but not in others,

and these samples were lost in the intersection dataset. Overall the abundance data are patchy, as these patients were likely all taking antibiotics for unrelated infections prior to CDI onset. A limitation of permutation importance is that the contribution of each feature is considered in isolation, but members of microbial communities interact and compete with each other, thus these complicated relationships are not well captured by permutation importance.

The full pragmatic severity model performed just as well as a prior EHR-based model trained on the day of diagnosis, demonstrating the potential utility of OTU-based models. In terms of the number needed to screen, the OTU-based pragmatic severity model outperformed a prior model of manually curated clinical variables, but not a model trained on EHR data extracted two days after diagnosis. While the attributable definition had a worse NNS for the OTU-based models, it did not perform worse than the prior curated model, and it may be the most clinically relevant as physician chart review increases confidence that positively-labelled severe outcomes are due to the CDI rather than other causes. Obtaining EHR data for the dataset in this study would allow a more direct comparison of the performance of models trained on OTUs, EHRs, or both, as well as extracting EHR data on the day of diagnosis rather than two days after.

However, it is not enough for models to perform well to justify deploying them in a clinical setting; benefit over current practices must be shown (30). Although no known treatment options have been shown to reduce the risk of severe CDI outcomes, fidaxomicin is promising due to its improved time to resolution and reduced recurrence. Despite its increased cost, fidaxomicin is also attractive as a preferential antibiotic option as vancomycin-resistant *Enterococcus* is on the rise and enterococci are known to worsen CDI (31, 32). We extended our analysis of clinical value to incorporate the number needed to treat for fidaxomicin alongside the predictive models in order to calculate the number needed to benefit. The NNB contextualizes model performance within clinical reality, as it combines both model performance and treatment effectiveness (23). A more robust analysis of clinical value would further consider the cost of treatment options versus the savings of averting severe outcomes across a range of decision thresholds, as economic disparities are a major barrier to treatment in the US (24). Cost-benefit analyses based on clinical trial data have reported that fidaxomicin may be as cost-effective as vancomycin as a treatment for initial CDI cases, largely due to the reduced risk of recurrence (33, 34). While our analysis of clinical value is only a proof-of-concept, if evidence emerges that new or existing treatments significantly reduce the risk of severe CDI, our results can be incorporated into future considerations of whether to build severity prediction models and what features should be incorporated. In practice, EHR-based models are less costly to deploy than OTU-based models and do not require additional clinical sample collection. Amplicon sequencing is not typically performed for CDI patients, however, routinely profiling the microbial communities of CDI patients could be justified if

models that incorporate microbial features were shown to improve patient outcomes.

In all, we found that our models to predict severity from features of the gut microbiome performed moderately well. Our approach enabled us to identify bacteria that contributed to model performance and evaluate how well the state of the gut microbiome can predict several different definitions of CDI severity. Further work is needed to determine whether the performance of OTU-based models is sufficient to justify their deployment in clinical settings, especially as compared to EHR-based models. If and when new evidence emerges of improved treatments to prevent severe CDI outcomes, deploying performant and robust models for clinicians to tailor treatment options may improve patient outcomes and reduce the burden of severe CDI.

MATERIALS AND METHODS

Sample collection. This study was approved by the University of Michigan Institutional Review Board. All patient samples were collected by the University of Michigan Health System from January 2016 through December 2017. Stool samples that had unformed stool consistency were tested for *C. difficile* by the clinical microbiology lab with a two-step algorithm that included detection of *C. difficile* glutamate dehydrogenase and toxins A and B by enzyme immunoassay with reflex to PCR for the *tcdB* gene when results were discordant. 1,517 stool samples were collected from patients diagnosed with a CDI. Leftover stool samples that were sent to the clinical microbiology lab were collected and split into different aliquots. For 16S sequencing, the aliquot of stool was re-suspended in DNA genotek stabilization buffer and then stored in the -80°C freezer.

16S rRNA gene amplicon sequencing. Samples stored in DNA genotek buffer were thawed from the -80°C, vortexed, and then transferred to a 96-well bead beating plate for DNA extractions. DNA was extracted using the DNeasy Powersoil HTP 96 kit (Qiagen) and an EpMotion 5075 automated pipetting system (Eppendorf). The V4 region of the 16S rRNA gene was amplified with the AccuPrime Pfx DNA polymerase (Thermo Fisher Scientific) using custom barcoded primers, as previously described (35). Each library preparation plate for sequencing contained a negative control (water) and mock community control (ZymoBIOMICS microbial community DNA standards). The PCR amplicons were normalized (SequalPrep normalization plate kit from Thermo Fisher Scientific), pooled and quantified (KAPA library quantification kit from KAPA Biosystems), and sequenced with the MiSeq system (Illumina).

All sequences were processed with mothur (v1.46) using the MiSeq SOP protocol (36, 35). Paired sequencing reads were combined and aligned with the SILVA (v132) reference database (37) and taxonomy was assigned with a modified

version of the Ribosomal Database Project reference sequences (v16) (38). Sequences were clustered into *de novo* OTUs with the OptiClust algorithm in mothur (39), resulting in 9,939 OTUs. Samples were then subsampled to 5,000 sequences per sample. Only the first CDI sample per patient was used for subsequent ML analyses such that no patient is represented more than once, resulting in a dataset of 1,277 samples.

Defining CDI severity. We chose to explore four different ways to define CDI cases as severe or not (Figure 1).

- **IDSA:** A case is severe if serum creatinine level is greater than or equal to 1.5mg/dL and the white blood cell count is greater than or equal to $15\text{k}/\mu\text{L}$ on the day of diagnosis (19).
- **All-cause:** A case is severe if ICU admission, colectomy, or death occurred within 30 days of CDI diagnosis, regardless of the cause of the adverse event.
- **Attributable:** A case is severe if an adverse event of ICU admission, colectomy, or death occurred within 30 days of CDI diagnosis, and the adverse event was determined to be attributable to the CDI by two physicians who reviewed the medical chart (21).
- **Pragmatic:** A case's severity is determined by the attributable definition if it is available, otherwise it is determined by the all-cause definition.

Model training. Random forest models were used to examine whether OTU data collected on the day of diagnosis could classify CDI cases as severe according to each severity definition. We used the mikropml R package v1.5.0 (40) implemented in a custom version of the mikropml Snakemake workflow (41) for all steps of the machine learning analysis. We have full datasets which use all samples available for each severity definition, and an intersection dataset which consists of only the samples that have all four definitions labelled. The intersection dataset is the most fair for comparing model performance across definitions, while the full dataset allows us to use as much data as possible for model training and evaluation. Datasets were pre-processed with the default options in mikropml to remove features with near-zero variance and scale continuous features from -1 to 1. During pre-processing, 9,757 to 9,760 features were removed due to having near-zero variance, resulting in datasets having 179 to 182 features depending on the severity definition. No features had missing values and no features were perfectly correlated. We randomly split the data into an 80% training and 20% test set and repeated this 100 times, followed by training models with 5-fold cross-validation.

Model evaluation. Model performance was calculated on the held-out test sets using the area under the receiver-operator characteristic curve (AUROC) and the area under the balanced precision-recall curve (AUBPRC). Permutation feature importance was then performed to determine which OTUs contributed most to model performance. We reported

OTUs with a significant permutation test in at least 75 of the 100 models.

Since the severity labels are imbalanced with different frequencies of severity for each definition, we calculated balanced precision, the precision expected if the labels were balanced. The balanced precision and the area under the balanced precision-recall curve (AUBPRC) were calculated with Equations 1 and 7 from Wu *et al.* (22).

Number needed to benefit. For the severity prediction models (which excludes the IDSA definition), we set out to estimate the potential benefit of deploying models in clinical settings. We determined the decision threshold at the 95th percentile of risk for each model, which corresponds to 5% of cases being predicted by the model to experience a severe outcome. At this threshold we computed the number needed to screen (NNS), which is the reciprocal of precision and represents the number of cases that must be predicted as severe to identify one true positive (42). The number needed to treat (NNT) is the number of true positive patients that must be treated by an intervention in order for one patient to benefit, and is calculated from the reciprocal of absolute risk in randomized controlled trials (43). Multiplying the NNS of a model by the NNT of a treatment yields the number needed to benefit (NNB) - the number of patients that must be predicted to have a severe outcome and undergo a treatment to benefit from it (23). NNB encapsulates the benefit of pairing a predictive model with a treatment in a clinical setting, with lower NNB numbers being better.

Code availability. The complete workflow, code, and supporting files required to reproduce this manuscript with accompanying figures is available at <https://github.com/SchlossLab/severe-CDI>.

The workflow was defined with Snakemake (44) and dependencies were managed with conda environments. Scripts were written in R (45), Python (46), and GNU bash. Additional software and packages used in the creation of this manuscript include cowplot (47), ggtext (48), ggsankey (49), schtools (50), the tidyverse metapackage (51), Quarto, and vegan (52).

Data availability. The 16S rRNA sequencing data have been deposited in the National Center for Biotechnology Information Sequence Read Archive (BioProject Accession no. PRJNA729511).

ACKNOWLEDGEMENTS

We thank the patients for donating stool samples and the research team members who collected, stored, and processed the samples.

297 REFERENCES

1. **Magill SS, Edwards JR, Bamberg W, Beldavs ZG, Dumyati G, Kainer MA, Lynfield R, Maloney M, McAllister-Hollod L, Nadle J, Ray SM, Thompson DL, Wilson LE, Fridkin SK.** Mar 2014. Multistate Point-Prevalence Survey of Health Care–Associated Infections. *N Engl J Med* 370 (13):1198–1208. doi:[10.1056/NEJMoa1306801](https://doi.org/10.1056/NEJMoa1306801).
2. **Feuerstadt P, Theriault N, Tillotson G.** Mar 2023. The Burden of CDI in the United States: A Multifactorial Challenge. *BMC Infect Dis* 23 (1):132. doi:[10.1186/s12879-023-08096-0](https://doi.org/10.1186/s12879-023-08096-0).
3. **Kelly CP.** Jan 2012. Can We Identify Patients at High Risk of Recurrent *Clostridium Difficile* Infection? *Clin Microbiol Infect* 18:21–27. doi:[10.1111/1469-0691.12046](https://doi.org/10.1111/1469-0691.12046).
4. **Janarthanan S, Ditah I, Adler DG, Ehrinpreis MN.** Jul 2012. *Clostridium Difficile*-Associated Diarrhea and Proton Pump Inhibitor Therapy: A Meta-Analysis. *Off journal Am Coll Gastroenterol | ACG* 107 (7):1001. doi:[10.1038/ajg.2012.179](https://doi.org/10.1038/ajg.2012.179).
5. **Tomkovich S, Taylor A, King J, Colovas J, Bishop L, McBride K, Royzenblat S, Lesniak NA, Bergin IL, Schloss PD.** Sep 2021. An Osmotic Laxative Renders Mice Susceptible to Prolonged *Clostridioides Difficile* Colonization and Hinders Clearance. *mSphere* 6 (5):10.1128/msphere.00629–21. doi:[10.1128/msphere.00629-21](https://doi.org/10.1128/msphere.00629-21).
6. **Lucado J, Elixhauser A.** 2012. *Clostridium Difficile* Infections (CDI) in Hospital Stays, 2009. HCUP Statistical Brief #124. AHRQ <http://www.hcup-us.ahrq.gov/reports/statbriefs/sb124.pdf>.
7. **Kassam Z, Cribb Fabersunne C, Smith MB, Alm EJ, Kaplan GG, Nguyen GC, Ananthakrishnan AN.** Mar 2016. *Clostridium Difficile* Associated Risk of Death Score (CARDS): A Novel Severity Score to Predict Mortality among Hospitalised Patients with *C. Difficile* Infection. *Aliment Pharmacol Ther* 43 (6):725–733. doi:[10.1111/apt.13546](https://doi.org/10.1111/apt.13546).
8. **Napolitano LM, Edmiston CE.** Aug 2017. *Clostridium Difficile* Disease: Diagnosis, Pathogenesis, and Treatment Update. *Surgery* 162 (2):325–348. doi:[10.1016/j.surg.2017.01.018](https://doi.org/10.1016/j.surg.2017.01.018).
9. **Ressler A, Wang J, Rao K.** Jan 2021. Defining the Black Box: A Narrative Review of Factors Associated with Adverse Outcomes from Severe *Clostridioides Difficile* Infection. *Ther Adv Gastroenterol* 14:17562848211048127. doi:[10.1177/17562848211048127](https://doi.org/10.1177/17562848211048127).
10. **Guh AY, Mu Y, Winston LG, Johnston H, Olson D, Farley MM, Wilson LE, Holzbauer SM, Phipps EC, Dumyati GK, Beldavs ZG, Kainer MA, Karlsson M, Gerding DN, McDonald LC.** Apr 2020. Trends in U.S. Burden of *Clostridioides Difficile* Infection and Outcomes. *N Engl J Med* 382 (14):1320–1330. doi:[10.1056/NEJMoa1910215](https://doi.org/10.1056/NEJMoa1910215).
11. **Kwon JH, Olsen MA, Dubberke ER.** Mar 2015. The Morbidity, Mortality, and Costs Associated with *Clostridium Difficile* Infection. *Infect Dis Clin North Am* 29 (1):123–134. doi:[10.1016/j.idc.2014.11.003](https://doi.org/10.1016/j.idc.2014.11.003).
12. **Chakra CNA, Pepin J, Valiquette L.** Jan 2012. Prediction Tools for Unfavourable Outcomes in *Clostridium Difficile* Infection: A Systematic Review. *PLOS ONE* 7 (1):e30258. doi:[10.1371/journal.pone.0030258](https://doi.org/10.1371/journal.pone.0030258).
13. **Perry DA, Shirley D, Micic D, Patel PC, Putler R, Menon A, Young VB, Rao K.** Jun 2022. External Validation and Comparison of *Clostridioides Difficile* Severity Scoring Systems. *Clin Infect Dis* 74 (11):2028–2035. doi:[10.1093/cid/ciab737](https://doi.org/10.1093/cid/ciab737).
14. **Rao K, Micic D, Natarajan M, Winters S, Kiel MJ, Walk ST, Santhosh K, Mogle JA, Galecki AT, LeBar W, Higgins PDR, Young VB, Aronoff DM.** Jul 2015. *Clostridium Difficile* Ribotype 027: Relationship to Age, Detectability of Toxins A or B in Stool With Rapid Testing, Severe Infection, and Mortality. *Clin Infect Dis* 61 (2):233–241. doi:[10.1093/cid/civ254](https://doi.org/10.1093/cid/civ254).
15. **Li BY, Oh J, Young VB, Rao K, Wiens J.** May 2019. Using Machine Learning and the Electronic Health Record to Predict Complicated *Clostridium*

- Difficile* Infection. Open Forum Infect Dis 6 (5):ofz186. doi:[10.1093/ofid/ofz186](https://doi.org/10.1093/ofid/ofz186).
16. **Tomkovich S, Stough JMA, Bishop L, Schloss PD.** Oct 2020. The Initial Gut Microbiota and Response to Antibiotic Perturbation Influence *Clostridioides Difficile* Clearance in Mice. mSphere 5 (5). doi:[10.1128/mSphere.00869-20](https://doi.org/10.1128/mSphere.00869-20).
 17. **Lesniak NA, Schubert AM, Flynn KJ, Leslie JL, Sinani H, Bergin IL, Young VB, Schloss PD.** Jul 2022. The Gut Bacterial Community Potentiates *Clostridioides Difficile* Infection Severity. mBio 13 (4):e01183–22. doi:[10.1128/mbio.01183-22](https://doi.org/10.1128/mbio.01183-22).
 18. **Dieterle MG, Putler R, Perry DA, Menon A, Abernathy-Close L, Perlman NS, Penkevich A, Standke A, Keidan M, Vendrov KC, Bergin IL, Young VB, Rao K.** May 2020. Systemic Inflammatory Mediators Are Effective Biomarkers for Predicting Adverse Outcomes in *Clostridioides Difficile* Infection. mBio 11 (3):e00180–20. doi:[10.1128/mBio.00180-20](https://doi.org/10.1128/mBio.00180-20).
 19. **McDonald LC, Gerding DN, Johnson S, Bakken JS, Carroll KC, Coffin SE, Dubberke ER, Garey KW, Gould CV, Kelly C, Loo V, Shaklee Sammons J, Sandora TJ, Wilcox MH.** Mar 2018. Clinical Practice Guidelines for *Clostridium Difficile* Infection in Adults and Children: 2017 Update by the Infectious Diseases Society of America (IDSA) and Society for Healthcare Epidemiology of America (SHEA). Clin Infect Dis 66 (7):e1–e48. doi:[10.1093/cid/cix1085](https://doi.org/10.1093/cid/cix1085).
 20. **Stevens VW, Shoemaker HE, Jones MM, Jones BE, Nelson RE, Khader K, Samore MH, Rubin MA.** May 2020. Validation of the SHEA/IDSA Severity Criteria to Predict Poor Outcomes among Inpatients and Outpatients with *Clostridioides Difficile* Infection. Infect Control & Hosp Epidemiol 41 (5):510–516. doi:[10.1017/ice.2020.8](https://doi.org/10.1017/ice.2020.8).
 21. **McDonald LC, Coignard B, Dubberke E, Song X, Horan T, Kutty PK.** 2007. Recommendations for Surveillance of *Clostridium Difficile*-Associated Disease. Infect Control & Hosp Epidemiol 28 (2):140–145. doi:[10.1086/511798](https://doi.org/10.1086/511798).
 22. **Wu Y, Liu H, Li R, Sun S, Weile J, Roth FP.** Oct 2021. Improved Pathogenicity Prediction for Rare Human Missense Variants. The Am J Hum Genet 108 (10):1891–1906. doi:[10.1016/j.ajhg.2021.08.012](https://doi.org/10.1016/j.ajhg.2021.08.012).
 23. **Liu VX, Bates DW, Wiens J, Shah NH.** Dec 2019. The Number Needed to Benefit: Estimating the Value of Predictive Analytics in Healthcare. J Am Med Informatics Assoc 26 (12):1655–1659. doi:[10.1093/jamia/ocz088](https://doi.org/10.1093/jamia/ocz088).
 24. **Johnson S, Laverne V, Skinner AM, Gonzales-Luna AJ, Garey KW, Kelly CP, Wilcox MH.** Sep 2021. Clinical Practice Guideline by the Infectious Diseases Society of America (IDSA) and Society for Healthcare Epidemiology of America (SHEA): 2021 Focused Update Guidelines on Management of *Clostridioides Difficile* Infection in Adults. Clin Infect Dis 73 (5):e1029–e1044. doi:[10.1093/cid/ciab549](https://doi.org/10.1093/cid/ciab549).
 25. **Long B, Gottlieb M.** 2022. Oral Fidaxomicin versus Vancomycin for *Clostridioides Difficile* Infection. Acad Emerg Med 29 (12):1506–1507. doi:[10.1111/acem.14600](https://doi.org/10.1111/acem.14600).
 26. **Tashiro S, Mihara T, Sasaki M, Shimamura C, Shimamura R, Suzuki S, Yoshikawa M, Hasegawa T, Enoki Y, Taguchi K, Matsumoto K, Ohge H, Suzuki H, Nakamura A, Mori N, Morinaga Y, Yamagishi Y, Yoshizawa S, Yanagihara K, Mikamo H, Kunishima H.** Nov 2022. Oral Fidaxomicin versus Vancomycin for the Treatment of *Clostridioides Difficile* Infection: A Systematic Review and Meta-Analysis of Randomized Controlled Trials. J Infect Chemother 28 (11):1536–1545. doi:[10.1016/j.jiac.2022.08.008](https://doi.org/10.1016/j.jiac.2022.08.008).
 27. **Schubert AM, Rogers MAM, Ring C, Mogle J, Petrosino JP, Young VB, Aronoff DM, Schloss PD.** Jul 2014. Microbiome Data Distinguish Patients with *Clostridium Difficile* Infection and Non-*C. Difficile*-Associated Diarrhea from Healthy Controls. mBio 5 (3). doi:[10.1128/mBio.01021-14](https://doi.org/10.1128/mBio.01021-14).
 28. **Antharam VC, Li EC, Ishmael A, Sharma A, Mai V, Rand KH, Wang GP.** Sep 2013. Intestinal Dysbiosis and Depletion of Butyrogenic Bacteria in *Clostridium Difficile* Infection and Nosocomial Diarrhea. J Clin Microbiol 51 (9):2884–2892. doi:[10.1128/JCM.00845-13](https://doi.org/10.1128/JCM.00845-13).

29. **Berkell M, Mysara M, Xavier BB, van Werkhoven CH, Monsieurs P, Lammens C, Ducher A, Vehreschild MJGT, Goossens H, de Gunzburg J, Bonten MJM, Malhotra-Kumar S.** Apr 2021. Microbiota-Based Markers Predictive of Development of *Clostridioides Difficile* Infection. *Nat Commun* 12 (1):2241. doi:[10.1038/s41467-021-22302-0](https://doi.org/10.1038/s41467-021-22302-0).
30. **Wiens J, Saria S, Sendak M, Ghassemi M, Liu VX, Doshi-Velez F, Jung K, Heller K, Kale D, Saeed M, Ossorio PN, Thadaney-Israni S, Goldenberg A.** Sep 2019. Do No Harm: A Roadmap for Responsible Machine Learning for Health Care. *Nat Med* 25 (9):1337–1340. doi: [10.1038/s41591-019-0548-6](https://doi.org/10.1038/s41591-019-0548-6).
31. **Poduval RD, Kamath RP, Corpuz M, Norkus EP, Pitchumoni CS.** Dec 2000. *Clostridium Difficile* and Vancomycin-Resistant Enterococcus: The New Nosocomial Alliance. *Off journal Am Coll Gastroenterol | ACG* 95 (12):3513. doi:[10.1111/j.1572-0241.2000.03291.x](https://doi.org/10.1111/j.1572-0241.2000.03291.x).
32. **Smith AB, Jenior ML, Keenan O, Hart JL, Specker J, Abbas A, Rangel PC, Di C, Green J, Bustin KA, Gaddy JA, Nicholson MR, Laut C, Kelly BJ, Matthews ML, Evans DR, Van Tyne D, Furth EE, Papin JA, Bushman FD, Erlichman J, Baldassano RN, Silverman MA, Dunny GM, Prentice BM, Skaar EP, Zackular JP.** Nov 2022. Enterococci Enhance *Clostridioides Difficile* Pathogenesis. *Nature* 611 (7937):780–786. doi: [10.1038/s41586-022-05438-x](https://doi.org/10.1038/s41586-022-05438-x).
33. **Jiang Y, Sarpong EM, Sears P, Obi EN.** Feb 2022. Budget Impact Analysis of Fidaxomicin Versus Vancomycin for the Treatment of *Clostridioides Difficile* Infection in the United States. *Infect Dis Ther* 11 (1):111–126. doi:[10.1007/s40121-021-00480-0](https://doi.org/10.1007/s40121-021-00480-0).
34. **Reveles KR, Backo JL, Corvino FA, Zivkovic M, Broderick KC.** 2017. Fidaxomicin versus Vancomycin as a First-Line Treatment for *Clostridium Difficile*–Associated Diarrhea in Specific Patient Populations: A Pharmacoeconomic Evaluation. *Pharmacother The J Hum Pharmacol Drug Ther* 37 (12):1489–1497. doi:[10.1002/phar.2049](https://doi.org/10.1002/phar.2049).
35. **Kozich JJ, Westcott SL, Baxter NT, Highlander SK, Schloss PD.** Sep 2013. Development of a Dual-Index Sequencing Strategy and Curation Pipeline for Analyzing Amplicon Sequence Data on the MiSeq Illumina Sequencing Platform. *Appl. Environ. Microbiol.* 79 (17):5112–5120. doi: [10.1128/AEM.01043-13](https://doi.org/10.1128/AEM.01043-13).
36. **Schloss PD, Westcott SL, Ryabin T, Hall JR, Hartmann M, Hollister EB, Lesniewski RA, Oakley BB, Parks DH, Robinson CJ, Sahl JW, Stres B, Thallinger GG, Van Horn DJ, Weber CF.** 2009. Introducing Mothur: Open-Source, Platform-Independent, Community-Supported Software for Describing and Comparing Microbial Communities. *Appl Environ Microbiol* 75 (23):7537–7541. doi:[10.1128/AEM.01541-09](https://doi.org/10.1128/AEM.01541-09).
37. **Quast C, Pruesse E, Yilmaz P, Gerken J, Schweer T, Yarza P, Peplies J, Glöckner FO.** Jan 2013. The SILVA Ribosomal RNA Gene Database Project: Improved Data Processing and Web-Based Tools. *Nucleic Acids Res* 41 (D1):D590–D596. doi:[10.1093/nar/gks1219](https://doi.org/10.1093/nar/gks1219).
38. **Cole JR, Wang Q, Fish JA, Chai B, McGarrell DM, Sun Y, Brown CT, Porras-Alfaro A, Kuske CR, Tiedje JM.** Jan 2014. Ribosomal Database Project: Data and Tools for High Throughput rRNA Analysis. *Nucl. Acids Res.* 42 (D1):D633–D642. doi:[10.1093/nar/gkt1244](https://doi.org/10.1093/nar/gkt1244).
39. **Westcott SL, Schloss PD.** Mar 2017. OptiClust, an Improved Method for Assigning Amplicon-Based Sequence Data to Operational Taxonomic Units. *mSphere* 2 (2):e00073–17. doi:[10.1128/mSphereDirect.00073-17](https://doi.org/10.1128/mSphereDirect.00073-17).
40. **Topçuoğlu BD, Lapp Z, Sovacool KL, Snitkin E, Wiens J, Schloss PD.** May 2021. Mikropml: User-Friendly R Package for Supervised Machine Learning Pipelines. *JOSS* 6 (61):3073. doi:[10.21105/joss.03073](https://doi.org/10.21105/joss.03073).
41. **Sovacool K, Lapp Z, Armour C, Lucas SK, Schloss P.** Jan. 2023. Mikropml Snakemake Workflow doi:[10.5281/zenodo.4759351](https://doi.org/10.5281/zenodo.4759351).
42. **Rembold CM.** Aug 1998. Number Needed to Screen: Development of a Statistic for Disease Screening. *BMJ* 317 (7154):307–312. doi: [10.1136/bmj.317.7154.307](https://doi.org/10.1136/bmj.317.7154.307).
43. **Laupacis A, Sackett DL, Roberts RS.** 1988. An Assessment of Clinically Useful Measures of the Consequences of Treatment. *New Engl J Med*

- 318 (26):1728–1733. doi:[10.1056/NEJM198806303182605](https://doi.org/10.1056/NEJM198806303182605).
44. **Köster J, Rahmann S.** Oct 2012. Snakemake — a Scalable Bioinformatics Workflow Engine. *Bioinformatics* 28 (19):2520–2522. doi:[10.1093/bioinformatics/bts480](https://doi.org/10.1093/bioinformatics/bts480).
 45. **R Core Team.** 2023. R: A Language and Environment for Statistical Computing. Vienna, Austria. <https://www.R-project.org/>.
 46. **Van Rossum G, Drake FL.** 2009. Python 3 Reference Manual | Guide Books <https://dl.acm.org/doi/book/10.5555/1593511>.
 47. **Wilke CO.** 2020. Cowplot: Streamlined Plot Theme and Plot Annotations for 'Ggplot2' <https://CRAN.R-project.org/package=cowplot>.
 48. **Wilke CO.** 2020. Ggtext: Improved Text Rendering Support for 'Ggplot2' <https://CRAN.R-project.org/package=ggtext>.
 49. **Sjoberg D.** 2022. Ggsankey: Sankey, Alluvial and Sankey Bump Plots <https://github.com/davidsjoberg/ggsankey>.
 50. **Sovacool K, Lesniak N, Lucas S, Armour C, Schloss P.** 2022. Schtools: Schloss Lab Tools for Reproducible Microbiome Research doi:[10.5281/zenodo.6540686](https://doi.org/10.5281/zenodo.6540686).
 51. **Wickham H, Averick M, Bryan J, Chang W, McGowan LD, François R, Grolemund G, Hayes A, Henry L, Hester J, Kuhn M, Pedersen TL, Miller E, Bache SM, Müller K, Ooms J, Robinson D, Seidel DP, Spinu V, Takahashi K, Vaughan D, Wilke C, Woo K, Yutani H.** Nov 2019. Welcome to the Tidyverse. *J Open Source Softw* 4 (43):1686. doi:[10.21105/joss.01686](https://doi.org/10.21105/joss.01686).
 52. **Oksanen J, Simpson GL, Blanchet FG, Kindt R, Legendre P, Minchin PR, O'Hara RB, Solymos P, Stevens MHH, Szoecs E, Wagner H, Barbour M, Bedward M, Bolker B, Borcard D, Carvalho G, Chirico M, Caceres MD, Durand S, Evangelista HBA, FitzJohn R, Friendly M, Furneaux B, Hannigan G, Hill MO, Lahti L, McGlinn D, Ouellette MH, Cunha ER, Smith T, Stier A, Braak CJFT, Weedon J.** 2023. Vegan: Community Ecology Package. <https://github.com/vegandevs/vegan>.

298 SUPPLEMENT

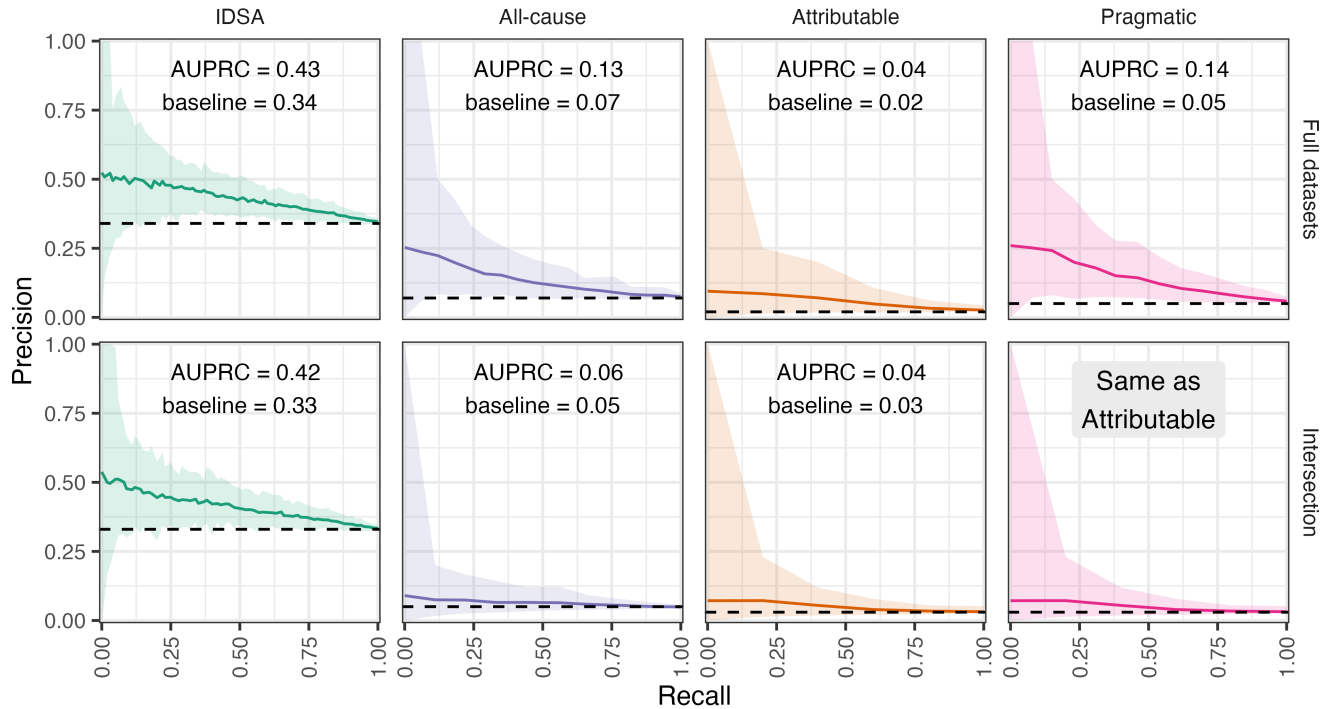


FIG 4 Precision-recall curves. The original precision-recall curves for each model. The horizontal line is the baseline precision, i.e. the proportion of severe cases in the dataset for each severity definition. Since each definition has a different baseline precision, the PRCs cannot be compared directly without balancing the precision (see Figure 2).

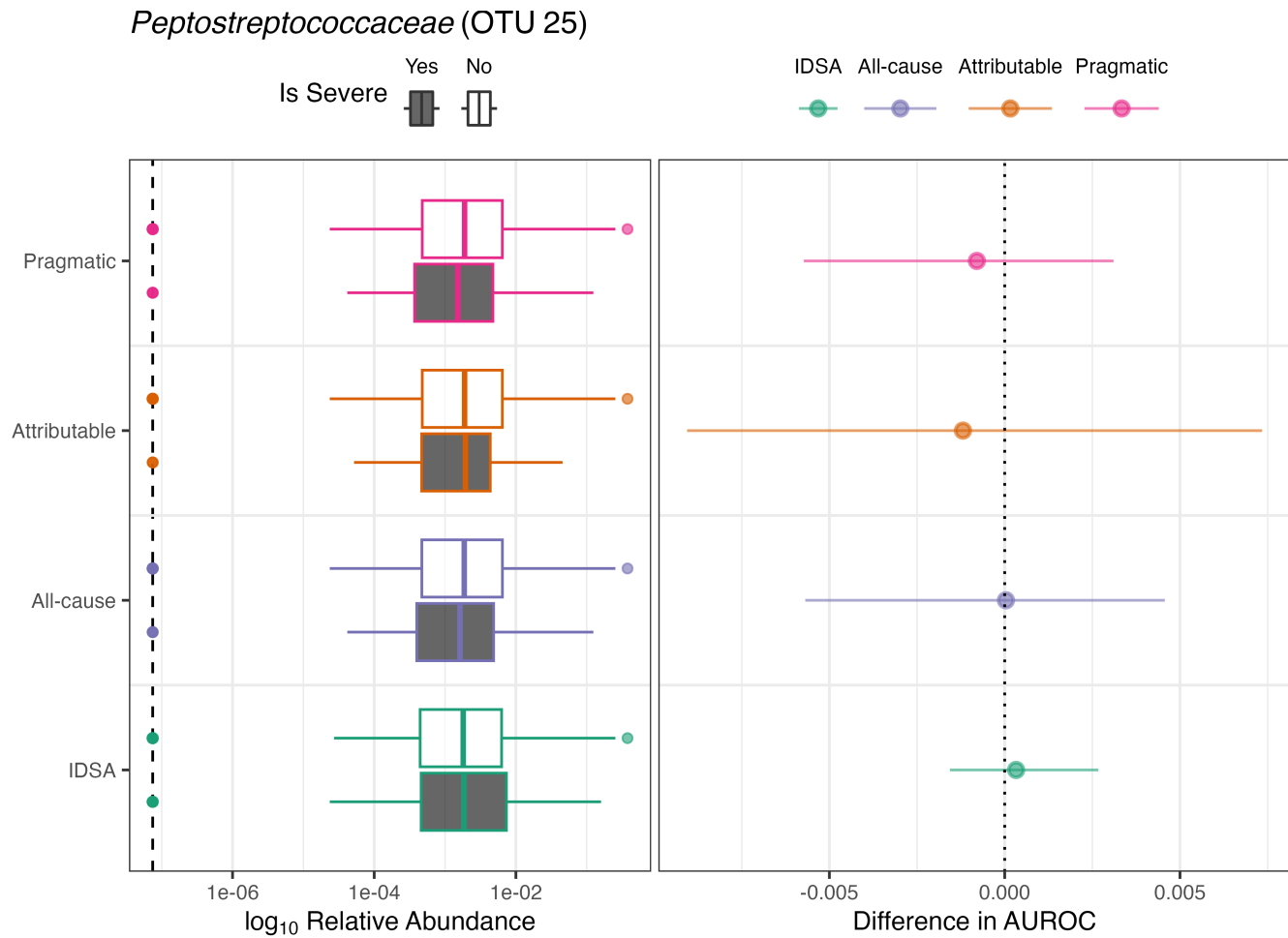


FIG 5 *C. difficile* relative abundance and feature importance. Of the 45 OTUs belonging to the *Peptostreptococcaceae* family, only one (OTU 25) had abundance values above the limit of detection. **Left:** \log_{10} -transformed relative abundance of OTU 25 in the full datasets. The dashed line is the limit of detection. **Right:** Permutation feature importance as measured by AUROC for OTU 25. The point is the mean difference in AUROC and the tails are the 75% confidence interval. The dotted line is a feature importance of zero, meaning the feature is not important.